Optimization of a Birefringence-Enhanced-Waveguide-Based Polarization Beam Splitter

Jong-Hoi Kim, Joong-Seon Choe, Chun-Ju Youn, Duk-Jun Kim, Yong-Hwan Kwon, and Eun-Soo Nam

We present the optimization of a birefringence-enhanced-waveguide (BWG)-based polarization beam splitter (PBS) in a Mach-Zehnder interferometer (MZI) configuration and analyze the structure-dependent or polarization-dependent phase difference, using a delay-line MZI (DL-MZI). We fabricate the DL-MZI using silica-based planar lightwave circuit technology and, using the DL-MZI, demonstrate the ability to optimize a PBS by measuring the birefringence of the BWG and structure-dependent phase offset.

Keywords: Polarization beam splitter, birefringence, planar lightwave circuit, monolithic integration, Mach-Zehnder interferometer, delay-line, and multimode interference coupler.

I. Introduction

Polarization beam splitting is one of the most essential functions for realizing a polarization multiplexed coherent optical transmission system that can offer high spectral efficiency, improvement in the optical signal-to-noise ratio, a large tolerance for chromatic and polarization-mode dispersions, and, in particular, mitigation of all electronic bandwidth requirements [1]. A polarization beam splitter (PBS) has recently become a key component in a dual-polarization quadrature phase-shift keying (DP-QPSK) transmission system. Integration with other components, such as an optical 90°-hybrid and balanced photodiode (BPD) is required since it is essential to provide lower cost and compactness for PBS implementation. In general, integration schemes are based on a monolithic or hybrid technology [2], [3]. For monolithic integration, InP-based coherent receivers comprising 90°-hybrids monolithically integrated with BPDs have been reported for 100G DP-QPSK transmission systems [4]-[6]. Furthermore, a monolithic silicon photonic integrated circuit (PIC), including two PBSs, two 90°-hybrids, and four pairs of BPDs implemented as integrated germanium detectors, has been realized [7]. An integrated PBS on a silica-based PLC that utilizes the waveguide birefringence dependence on the waveguide core width has been reported [8], and a compact dual-polarization optical hybrid with the integration of two PBSs and two 90°-hybrids has been demonstrated [9]. Silica-based planar lightwave circuit (PLC) technology, including monolithic or hybrid integration, has attracted significant attention as an alternative, owing to a low insertion loss and high reliability. An integrated PBS using silica-based PLC technology is required for commercial use in a DP-QPSK transmission system.

In this letter, we describe a delay-line Mach-Zehnder interferometer (DL-MZI) to measure the birefringence of the birefringence-enhanced waveguide (BWG) and structure-dependent phase offset. In addition, we show how the DL-MZI can be utilized to optimize a BWG-based PBS in an MZI configuration.

II. DL-MZI

To measure the birefringence of the BWG, a DL-MZI is fabricated on a Si substrate using silica-based PLC technology. The Si substrate consists of a BWG, a DL, and multimode interference (MMI) couplers. Birefringence of a silica-based waveguide on a Si substrate is enhanced by increasing its width, owing to the stress dependence on the waveguide core width

Manuscript received May 3, 2012; revised Aug. 16, 2012; accepted Aug. 22, 2012.
This work was partially supported by the IT R&D Program of KCC/KCA (08913-05003), Rep. of Korea.
Jong-Hoi Kim (phone: +82 42 860 6943, jonghoi@etri.re.kr), Joong-Seon Choe (jschoe@etri.re.kr), Chun-Ju Youn (cjyoun@etri.re.kr), Duk-Jun Kim (djkim@etri.re.kr), Yong-Hwan Kwon (yhkwon@etri.re.kr), and Eun-Soo Nam (esnam@etri.re.kr) are with the Convergence Components & Materials Research Laboratory, ETRI, Daejeon, Rep. of Korea.
http://dx.doi.org/10.4218/etrij.12.0212.0186

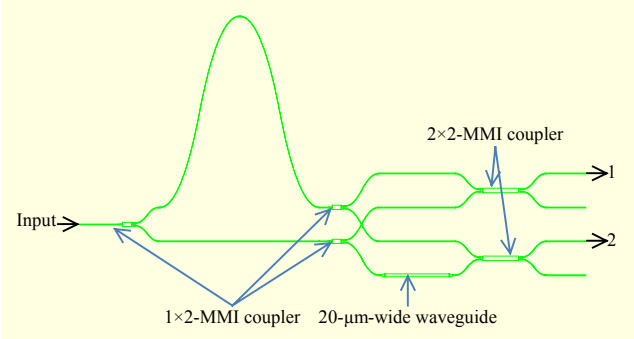

Fig. 1. Schematic diagram of DL-MZI.

[10]. A BWG is useful for realizing a PBS when designed to provide a phase difference of π between the transverse electric (TE) mode and the transverse magnetic (TM) mode. Waveguide birefringence can be estimated by measuring the phase differences between the TE and TM modes with the length of a given waveguide.

Figure 1 shows a schematic diagram of a DL-MZI for measuring the phase difference. The DL-MZI consists of two MZIs with a shared DL. The DL-MZI is fabricated on a Si substrate with a relative refractive index difference Δ of 0.75% and a waveguide core size of 6 μm × 6 μm using silica-based PLC technology. One of the MZIs includes a 20-μm-wide BWG designed to be expanded from a 6-μm-wide single-mode waveguide (SWG) using tapered waveguides to increase the birefringence. The other is used as a reference for measuring the phase offset occurring between output ports 1 and 2, owing to a structural difference in the waveguides. The free spectral range (FSR) of the DL-MZI is designed to be 400 GHz corresponding to a wavelength spacing of 3.2 nm at a wavelength of 1,550 nm.

III. Optimization

1. Birefringence-Enhanced Waveguide

For the measurement, the TE and TM polarized lights from an erbium-doped fiber amplifier (EDFA) are introduced into the input port of the DL-MZI and divided into the straight waveguide and bending waveguide for the delay. Once again, the light from the straight waveguide is divided into two paths through a 1×2-MMI coupler and then injected into the MZIs. Similarly, the light from the bending waveguide is coupled into the MZIs. In each MZI, the lights are combined in a 2×2-MMI coupler. As a result, the output powers from the ports of the DL-MZI show periodic peaks and valleys owing to constructive and destructive interferences with the wavelength spacing corresponding to the FSR. The phase difference between the TE and TM modes is then calculated using the phase difference between the output phases from the MZIs.

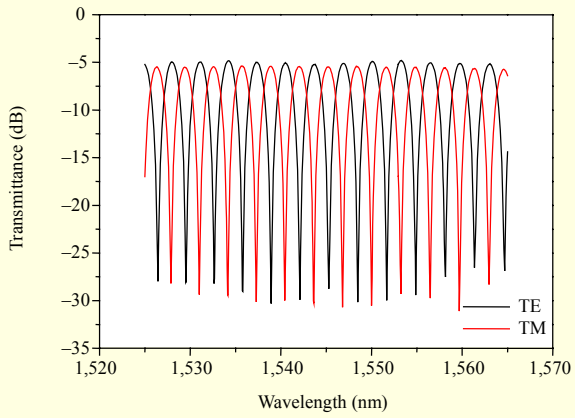

Fig. 2. Transmittance spectra from output port 2 of DL-MZI with 3-mm-long BWG.

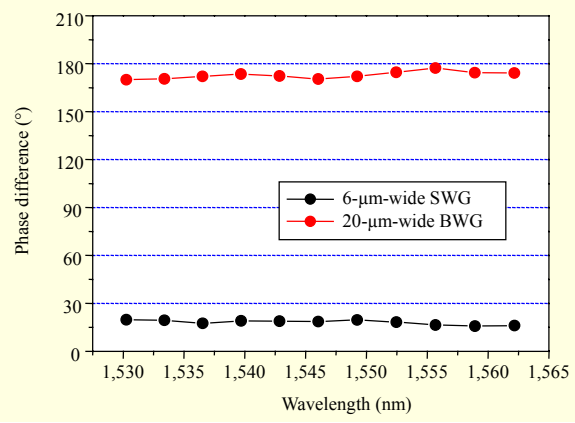

Fig. 3. Phase difference between TE and TM modes for 6-μm-wide SWG and 20-μm-wide BWG with length of 3 mm.

Using a wavelength spacing of $\Delta\lambda_P$ between the TE and TM modes and a wavelength spacing of $\Delta\lambda_F$ corresponding to the FSR, the phase difference $\Delta\theta$ between the TE and TM modes is approximately given by $2\pi\Delta\lambda_P/\Delta\lambda_F$.

Figure 2 shows the transmittance spectra from output port 2 of the DL-MZI for the TE and TM modes propagating through the BWG. Thus, the phase difference between the TE and TM modes is calculated from $\Delta\lambda_P$ and $\Delta\lambda_F$. For the 3-mm-long BWG, the wavelength spacing of $\Delta\lambda_P$ and $\Delta\lambda_F$ are 1.7 nm and 3.18 nm, respectively. Using all of the valleys in the transmittance spectra, the phase differences over a wavelength range of more than 30 nm can be measured. Figure 3 shows the phase differences for the 3-mm-long BWG and the SWG, which are symmetrically placed in the arms of the DL-MZI. The phase differences for the BWG are in the range of 170° to 177° over a wavelength range of 1,530 nm to 1,565 nm, while the SWG shows a phase difference of 16° to 20°.

For realizing a PBS with a high polarization extinction ratio (PER), a phase difference of π between TE and TM modes

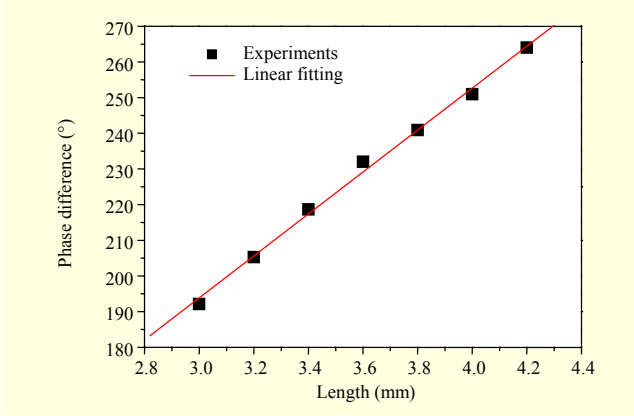

Fig. 4. Phase difference between TE and TM modes with BWG length.

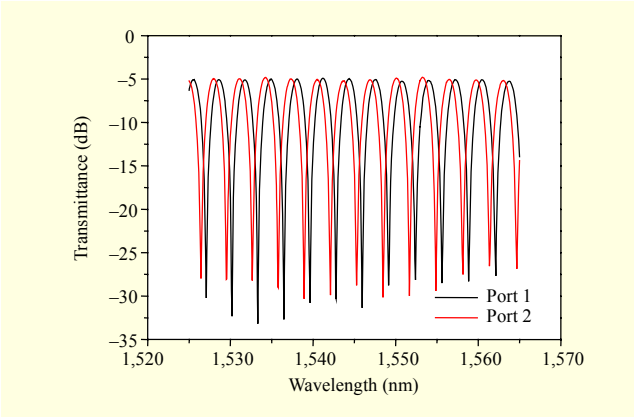

Fig. 5. Transmittance spectra of TE mode from outputs ports 1 and 2 of DL-MZI with 3-mm-long BWG.

propagating through the BWG can be achieved by optimizing the length of the BWG. Figure 4 shows the measured phase difference between the TE and TM modes with the length of the BWG using the transmission spectra from output port 2 of the DL-MZI. Note that birefringence Δn is based on the ratio $\Delta\theta/\Delta L$ of the phase difference to the length of the BWG and is given simply by $\lambda\Delta\theta/2\pi\Delta L$.

As a result, the ratio $\Delta\theta/\Delta L$ is 58.8° mm^{-1}, and, thus, a birefringence of 2.53×10^{-4} is obtained using the destructive interference valleys near a wavelength of 1,550 nm in the transmission spectra. From the results of the linear fitting, the phase shift owing to the tapered waveguides connected to the BWG is calculated as 17.7°. The BWG length for achieving the phase difference of π between the TE and TM modes is optimized using the measured birefringence and is expected to be 3.1 mm long from the results.

2. Structure-Dependent Phase Offset

The structural difference between the SWG and BWG can induce a phase offset between the lights propagating through the arms. In the DL-MZI, the phase offset is equivalent to the phase difference between output ports 1 and 2. Figure 5 shows the transmittance spectra for the TE mode from output ports 1 and 2 of the DL-MZI with the 3-mm-long BWG.

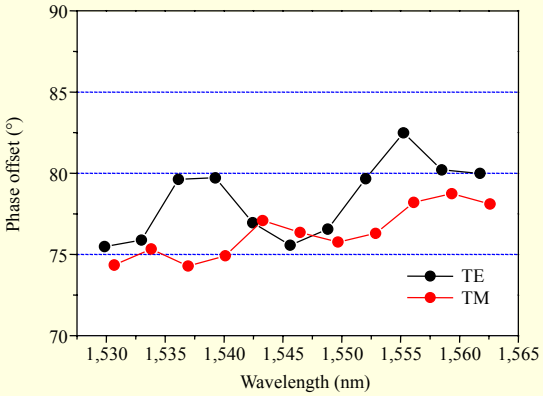

Fig. 6. Measured phase offset for DL-MZI with 3-mm-long BWG.

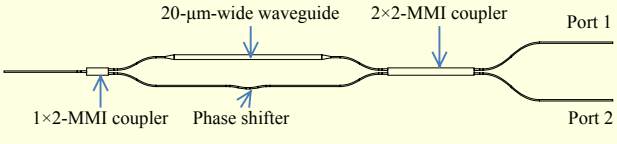

Fig. 7. Fabricated PBS.

Considering a phase difference of $\pi/2$ between two outputs from a 2×2-MMI coupler, the phase offset should be $\pi/2$ and $-\pi/2$ for complete constructive and destructive interference and vice versa for polarization beam splitting. As shown in Fig. 6, the phase offset is dependent on the wavelength and is about 76° at a wavelength of around 1,550 nm. Thus, a phase shifter is required to compensate the phase offset.

3. Silica-PLC-Based PBS

Based on the optimization of the BWG and the measurement of the phase offset, a PBS based on an MZI is fabricated using a silica-based PLC on a Si substrate, consisting of a 1×2-MMI coupler for dividing into two arms in the MZI, a 20-μm-wide and 3.1-mm-long BWG, a phase shifter of a bending SWG for compensating the phase offset, and a 2×2-MMI coupler, as shown in Fig. 7. The polarization mode of the light from each output port is determined by the phase offset in the phase shifter. For measuring a PER, the EDFA light source is introduced into the input port, and the polarized light powers are measured in each output port using a polarizer. Here, the TE mode is dominant in port 1, and the TM mode is dominant in port 2.

Figure 8 shows PERs of more than 17 dB and 25 dB for TE-

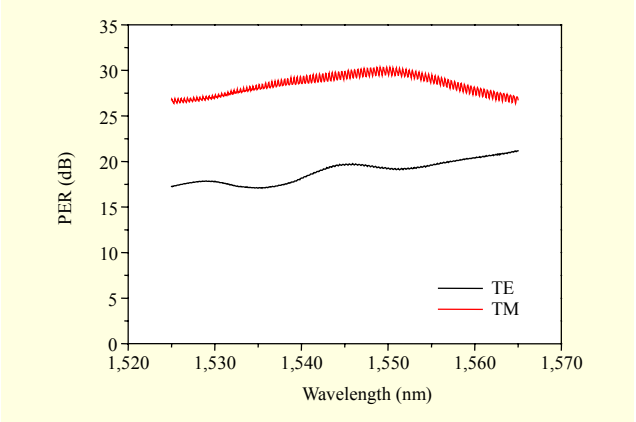

Fig. 8. PERs for TE- and TM-polarization of PBS.

polarization and TM-polarization, respectively, of over a wavelength range of 1,525 nm to 1,565 nm. When a phase difference between two output ports of a 2×2-MMI coupler is closer to $\pi/2$, the interference in one of the two ports is more constructive and, in the other, more destructive. Thus, the PER is higher. The 2×2-MMI in the DL-MZI shows a phase difference of 87° between the two output ports, and, consequently, the PER for both polarization states is degraded overall. We expect that the PER is improved by optimizing a length of the 2×2-MMI.

IV. Conclusion

We measured the waveguide birefringence and phase offset using a DL-MZI for optimizing a PBS. The DL-MZI was fabricated on a Si substrate using silica-based PLC technology, consisting of a BWG, MZIs with a shared DL, and MMI couplers. Using the device, the phase differences between the TE and TM modes based on the length of the BWG and the phase offset between lights propagating through the SWG and BWG were measured. We also showed the ability to optimize a BWG-based PBS in an MZI configuration.

References

[1] M. Birk et al., "Coherent 100 Gb/s PM-QPSK Field Trial," *IEEE Commun. Mag.*, vol. 48, no. 7, 2010, pp. 52-60.

[2] O.K. Kwon et al., "InP-Based Polarization-Insensitive Planar Waveguide Concave Grating Demultiplexer with Flattened Spectral Response," *ETRI J.*, vol. 31, no. 2, Apr. 2009, pp. 228-230.

[3] J.U. Shin et al., "Reconfigurable Optical Add-Drop Multiplexer Using a Polymer Integrated Photonic Lightwave Circuit," *ETRI J.*, vol. 31, no. 6, Dec. 2009, pp. 770-777.

[4] A. Matiss et al., "Performance of an Integrated Coherent Receiver Module for up to 160G DP-QPSK Transmission Systems," *J. Lightw. Technol.*, vol. 29, no. 7, 2011, pp. 1026-1032.

[5] V. Houtsma et al., "Manufacturable Monolithically Integrated InP Dual-Port Coherent Receiver for 100G PDM-QPSK Applications," *OFC*, 2011, OML2.

[6] R. Nagarajan et al., "10 Channel, 100Gbit/s per Channel, Dual Polarization, Coherent QPSK, Monolithic InP Receiver Photonic Integrated Circuit," *OFC*, 2011, OML7.

[7] C.R. Doerr et al., "Monolithic Polarization and Phase Diversity Coherent Receiver in Silicon," *J. Lightw. Technol.*, vol. 28, no. 4, 2010, pp. 520-525.

[8] Y. Sakamaki et al., "Dual Polarisation Optical Hybrid Using Silica-based Planar Lightwave Circuit Technology for Digital Coherent Receiver," *Electron. Lett.*, vol. 46, no. 1, 2010, pp. 58-60.

[9] T. Ohyama et al., "All-in-One 100-Gbit/s DP-QPSK Coherent Receiver Using Novel PLC-Based Integration Structure with Low-Loss and Wide-Tolerance Multi-channel Optical Coupling," *OECC*, 2010, PD6.

[10] Y. Hashizume et al., "Integrated Polarization Beam Splitter Using Waveguide Birefringence Dependence on Waveguide Core Width," *Electron. Lett.*, vol. 37, no. 25, 2001, pp. 1517-1518.